UTILIZATION OF AIRBORNE AND IN SITU DATA OBTAINED IN SGP99, SMEX02, CLASIC AND SMAPVEX08 FIELD CAMPAIGNS FOR SMAP SOIL MOISTURE ALGORITHM DEVELOPMENT AND VALIDATION

Andreas Colliander[1], Steven Chan[1], Simon Yueh[1], Michael Cosh[2], Rajat Bindlish[2], Tom Jackson[2], Eni Njoku[1]

1) Jet Propulsion Laboratory, California Institute of Technology
2) USDA ARS Hydrology and Remote Sensing Lab

ABSTRACT

Field experiment data sets that include coincident remote sensing measurements and in situ sampling will be valuable in the development and validation of the soil moisture algorithms of the NASA's future SMAP (Soil Moisture Active and Passive) mission. This paper presents an overview of the field experiment data collected from SGP99, SMEX02, CLASIC and SMAPVEX08 campaigns. Common in these campaigns were observations of the airborne PALS (Passive and Active L- and S-band) instrument, which was developed to acquire radar and radiometer measurements at low frequencies. The combined set of the PALS measurements and ground truth obtained from all these campaigns was under study. The investigation shows that the data set contains a range of soil moisture values collected under a limited number of conditions. The quality of both PALS and ground truth data meets the needs of the SMAP algorithm development and validation. The data set has already made significant impact on the science behind SMAP mission. The areas where complementing of the data would be most beneficial are also discussed.

Index Terms— Soil moisture, SMAP (Soil Moisture Active and Passive), SGP99, SMEX02, CLASIC, SMAPVEX08, PALS

1. INTRODUCTION

The NASA Soil Moisture Active and Passive (SMAP) mission is dedicated to measurement of global soil moisture and boreal land surface freeze/thaw state [1]. The satellite will carry radar (active) and radiometer (passive) L-band instruments that will perform simultaneous and coincident measurements of the Earth's surface. The combination of data from the two instruments will allow unprecedented accuracy, spatial resolution and temporal frequency for global mapping of soil moisture and freeze/thaw state.

Field experiment data sets that include coincident remote sensing measurements and in situ sampling will be valuable in the development and validation of SMAP soil moisture retrieval algorithms. Several candidate field experiment campaigns were carried out in the United States between 1999 and 2008 using the airborne Passive and Active L- and S-band (PALS) instrument [2]. These included SGP99 in Oklahoma in 1999 [3]; SMEX02 in Iowa in 2002 [4]; CLASIC in Oklahoma in 2007, and SMAPVEX08 in Maryland in 2008. The PALS instrument is a simulator for SMAP in that it includes both passive and active L-band sensors viewing at 40-degree incidence angle. The field campaign data sets include extensive sampling of ground conditions, including soil moisture, soil temperature, vegetation parameters and surface roughness along with soil texture, land cover and crop classification.

Previous papers have presented analyses of these field campaign data (e.g. [5] and [6] on SGP99, [7] on SMEX02, [8] and [9] on CLASIC and [10] on SMAPVEX08), but the data from all experiments have not been analyzed and intercompared as a combined set for soil moisture retrieval algorithm development. In this study the overall statistics of the experiment data and ground conditions of the abovementioned campaigns are presented. Furthermore, the consistency and characteristics of the data is evaluated. Finally, the value and impact of the data for SMAP algorithm validation is assessed and future needs of field experiments in light of these data are discussed.

2. FIELD EXPERIMENTS

In the following subsections short descriptions of the four field experiments are given.

2.1. SGP99

The SGP99 (1999 Southern Great Plains) experiment [3] in Oklahoma in July 8-14, 1999 was designed to study remote sensing of soil moisture in vegetated terrain. The study aimed to use L-, S- and C-band airborne observations and satellite observations with well characterized ground conditions. The PALS flights were conducted on six days. The landscape of the Little Washita watershed consisted of bare fields (harvested winter wheat), crops (alfalfa and corn), pasture (grasslands) and isolated forested areas. A rainstorm during the experiment on July 10 allowed observations of wetting and drying conditions.

2.2. SMEX02

The SMEX02 (Soil Moisture Experiments in 2002) experiment [4] in Iowa in June 25-July 8, 2002 was designed to investigate algorithms for soil moisture retrieval from microwave radars and radiometers under dense vegetation conditions. Specifically, the experiment also aimed at validation of soil moisture retrievals produced by the spaceborne AMSR-E microwave radiometer. The PALS flights were carried out on 8 days. The terrain of Walnut Creek watershed is undulating and the cover type for the region is primarily agricultural with corn and soybeans being the dominant crops. Scattered thunderstorms during the experiment on July 4, 5 and 6 enabled observation of wetting and drying conditions.

2.3. CLASIC

The CLASIC (Cloud and Land Surface Interaction Campaign) experiment took place in Oklahoma in June 11-July 6, 2007. This cross-disciplinary interagency research effort was designed to advance the understanding of how land surface processes influence cumulus convection. The PALS observations were one part of CLASIC with aim to collect radar and radiometer data for combined algorithm development for SMAP type concept. The PALS flights were conducted on 10 days. The landscape was similar to SGP99 with addition of region close to Fort Cobb. Heavy rainfall took place during the campaign which resulted in very wet conditions for the experiment.

2.4. SMAPVEX08

The SMAPVEX08 (SMAP Validation Experiment 2008) took place in Maryland in September 29-October 13, 2008. The experiment was designed to answer specific soil moisture algorithm and RFI mitigation questions related to L-band remote sensing. The PALS flights were carried out on 7 days. The experiment was focused on Choptank study area, which is defined by mixed agriculture fields and forest. The major crops are corn and soybean and the forests are mostly deciduous. A rain event on September 30, 2008 allowed observation of varying soil moisture conditions.

3. DATA DESCRIPTION

In the following subsections an overview of the ground truth, PALS measurements and spatial extent of all campaigns are given, and overall statistics of the measured parameters are presented.

3.1. Ground truth overview

The analyzed field campaigns produced 1033 samples of ground truth records of various parameters. However, not all parameters were sampled at each point on each day for a given campaign. There are 795 samples of surface soil moisture in the data set. The records were accumulated from 125 individual fields in all campaigns.

The prominent vegetation parameter sampled in all campaigns was Vegetation Water Content (VWC). Other sampled vegetation parameters include biomass, and Leaf Area Index (LAI). In situ sampled VWC is associated with 411 records. For determining VWC over the each observed spatial domain NDWI (Normalized Difference Water Index) obtained from optical satellite imagery was utilized. The in situ sampled VWC was used to calibrate the satellite retrievals. VWC retrieved either in situ or through NDWI is associated with 913 records.

The surface roughness was determined using photographs of grid boards showing the profile of the surface. In some cases the roughness parameters RMS (Root Mean Square) height variation and correlation length was determined in two perpendicular orientations. The roughness parameters are associated with 431 ground truth records.

The physical temperature of the surface was measured at three depths: the skin with infrared measurement, 1 cm depth and 5 cm depth. These temperatures are associated with 736 ground truth records.

3.2. PALS measurement overview

The PALS instrument was deployed on multiple days in each campaign. The configuration of the instrument changed from campaign to campaign, but the basic performance parameters remained the same throughout all campaigns. In SGP99 and SMEX02 PALS flew on a C-130 aircraft operated by NCAR. In CLASIC and SMAPVEX08 it flew on a Twin Otter (DHC-6) aircraft. In SGP99 and SMEX02 PALS was using a horn antenna with 13° beamwidth, but in CLASIC and SMAPVEX08 the next generation design incorporated a lightweight microstrip antenna (which allowed the installation to the Twin Otter) with 20° beamwidth. Additionally, in SMAPVEX08 PALS was flown with an Agile Digital Detector (ADD) for RFI mitigation [10]. The resolution of PALS radiometer and radar have remained in <0.2 K and <0.2 dB range throughout the campaigns.

3.3. Spatial extent

The PALS instrument was used to map each experiment domain several times over the course of each campaign providing coverage beyond the measurements over the in situ sites. The ancillary data associated with each of the complete domain include infrared temperature (airborne measurement), VWC (optical satellite imagery), soil texture (soil databases) and land use classification (optical satellite imagery). Table 1 shows the spatial extent of each mapped domain, the number of flights conducted over the domain and the number of in situ sites distributed over each domain.

Table 1. Spatial extent of the experiment domains, number of flights and number of in situ sites at each domain.

Campaign	Watershed	Area [km]	Flights	In situ sites
SGP99	Little Washita	7x41	5	23
SMEX02	Walnut Creek	7x35	8	31
CLASIC	Little Washita Fort Cobb	6x52 3x28	8 10	15 13
SMAPVEX08	Choptank	7x55	7	43

3.4. Overall statistics

Figure 1 shows the histogram of sampled soil moisture in nominally 0-6 cm layer (in SGP99 0-5 cm layer was measured) using a soil moisture probe (except SGP99 where only gravimetric method was used). The histogram shows a high number of samples in 0.05 to 0.35 cm^3/cm^3 range and especially large number between 0.20 and 0.25 cm^3/cm^3. As the typical maximum soil water content is around 0.40 cm^3/cm^3 it can be concluded that the data provide extensive range of soil moisture values.

Figure 2 shows the histogram of the VWC measurements. For SMEX02 VWC was interpolated for each day using NDWI images obtained on different days. For the other campaigns a constant VWC map was used for each day of the campaign. Low VWC (<1 kg/m^2) is clearly dominating but higher VWC values up to 5 kg/m^2 and more are also present in substantial numbers in the data set.

Figure 3 displays the histograms of the effective roughness and correlation length of the surface. The effective parameters take the RMS value of the available roughness parameters of the given location to illustrate the general roughness conditions at that location. The histogram shows that roughness conditions were relatively similar in all campaigns.

Figure 4 shows the distribution of land cover types of all 1033 samples obtained from all campaigns. Figure 4 also shows the distribution of the crop types for the measurement sites classified as croplands. Agricultural regions clearly dominate the land cover distribution.

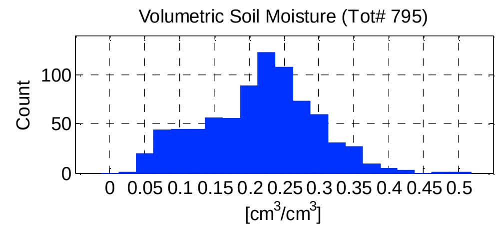

Figure 1. Volumetric soil moisture histogram based on the ground sampling. The total number of samples is shown in the parenthesis.

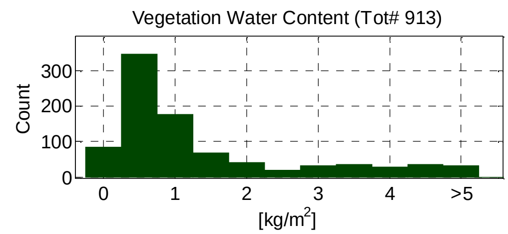

Figure 2. Vegetation water content histogram based on both ground sampling and remote sensing (NDWI).

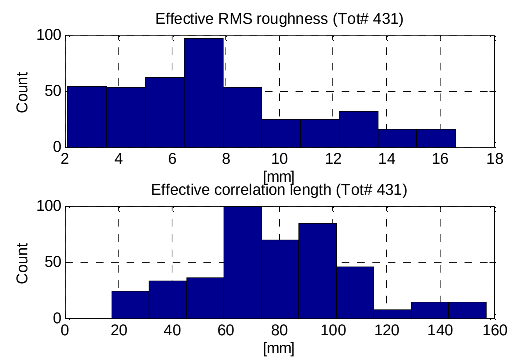

Figure 3. Histograms of effective roughness and correlation length of the surface.

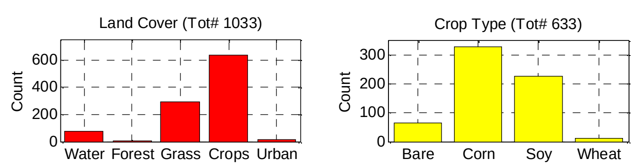

Figure 4. Land cover histogram based on remote sensing classification based on optical satellite data (left) and crop type histogram for the 633 samples of croplands (right).

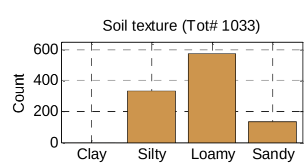

Figure 5. Soil texture histogram (based on soil data bases).

Finally, Figure 5 shows the distribution of soil texture. For illustration a rough classification is used to divide the soils in Clay (Clay percentage >50%), Silty (Silt percentage >50%), Loamy (Clay, Silt and Sand < 50%) and Sandy (Sand percentage >50%). The loamy soil type is the dominant throughout the combined data set.

Table 2 shows the brightness temperature (TB) and normalized radar cross-section (σ^0) ranges over land in the combined data set. The values of both instruments extend the expected range. Furthermore, the values represent significant fraction of physically possible brightness temperature and radar cross-section range from land surface.

Table 2. The range of radiometer and radar measurements.

	MIN	MAX	Range	Unit
TB V	208	294	86	K
TB H	165	285	120	K
σ^0 vv	-25.2	-3.3	21.9	dB
σ^0 hh	-25.1	-3.5	21.6	dB
σ^0 vh & hv	-37.0	-14.2	22.8	dB

4. DATA CHARACTERISTICS

The following subsections describe data calibration and consistency aspects of both ground truth and PALS measurements.

4.1. Calibration and consistency: ground truth

The ground truth sampling strategy varied somewhat from campaign to campaign depending on the objectives, approach and resources.

In the campaigns both gravimetric method and soil moisture probes were used to determine the soil water content. The value obtained through the gravimetric method is considered as the truth and was used to calibrate the probe measurement where available. Figure 6 (a) shows a comparison between the soil moisture obtained with the two methods. The data points include measurements from all other campaigns except SGP99, since the soil moisture probes were not utilized in SGP99. The calibration of the probe measurements is apparently very consistent and bias-free with RMSE of 0.02 cm^3/cm^3, which indicates high reliability of the samples.

Figure 6 (b) shows a comparison between VWC obtained from in situ sampling and VWC derived from NDWI. The in situ sampling is considered as the truth and was used to calibrate the NDWI derived VWC. The data points include samples from SMEX02 and SMAPVEX08 only, since for SGP99 the optical satellite data have not been processed and for CLASIC the in situ samples have not been completely processed. The agreement is bias-free with RMSE of 0.58 kg/m^2, which gives a good basis for VWC determination over the experiment domains.

The measurements of the physical temperature of the surface of the in situ sites were compared to each other. Figure 6 (c) shows a scatter plot of the skin temperature and soil temperature at 5 cm depth against soil temperature at 1 cm depth. As expected the temperature at 5 cm depth is cooler than at 1 cm depth at high temperature and the skin temperature is warmer with more dispersion than the subsurface temperatures. The comparison demonstrates the measured temperatures provide reliable means for computing the effective surface temperature for emissivity determination.

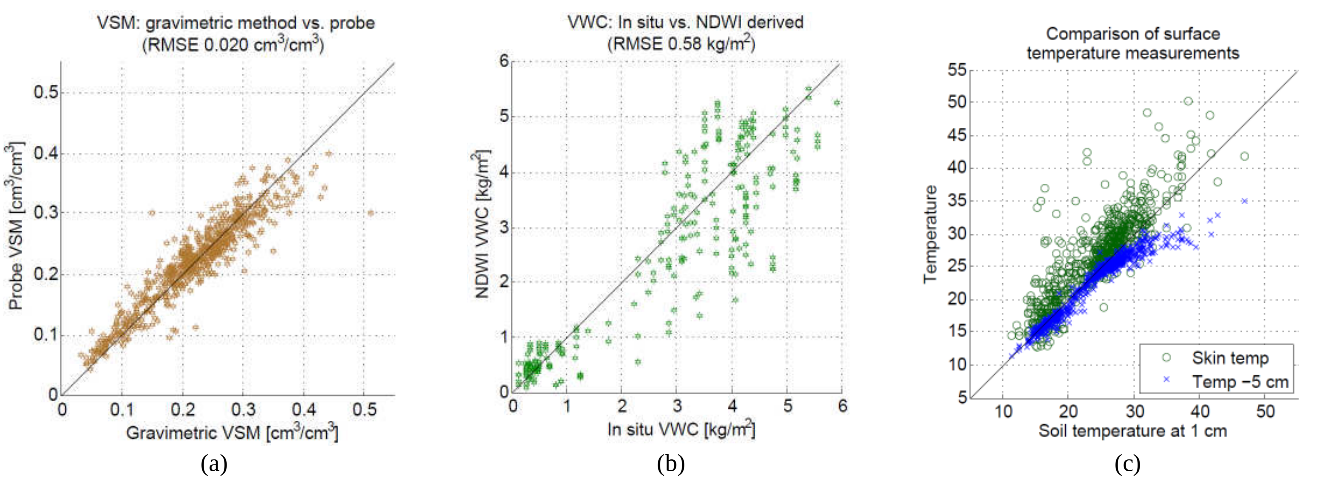

Figure 6. (a) Comparison between measurement of volumetric soil moisture (VSM) using the gravimetric method and a probe. Data from SMEX02, CLASIC and SMAPVEX08 are presented. (b) Comparison between measurement of VWC using in situ samples and satellite based NDWI. Data from SMEX02 and SMAPVEX08 are included. (c) Comparison of different surface temperature measurements. The skin temperature and the temperature at 5 cm depth are plotted against the temperature at1cm depth.

4.2. Calibration and consistency: PALS measurements

The calibration of the PALS instrument utilized a water body, either a lake or reservoir, selected for each campaign for the absolute calibration of brightness temperatures. The Klein and Swift model together with the water temperature obtained from the aircraft IR measurements or in-situ observations was used to estimate the water brightness temperatures at the PALS incidence angle for the calibration reference.

In order to investigate the consistency of brightness temperature and normalized radar cross-section values obtained with PALS measurements fields with nearly bare surfaces were selected from each campaign. The fields were selected based on photographs taken during the ground sampling and field notes. They included e.g. entirely bare crop fields and soy bean fields with very small plants. Figure 7 shows the brightness temperature values and Figure 8 shows the radar cross-section as a function of volumetric soil moisture of these fields (black crosses). The dominant degree of soil water content changed from campaign to campaign (see Section 2) and this is reflected also in this plot: the measurement points with VSM less than 0.25 are mostly from SGP99 and SMEX02, the measurement points with VSM between 0.20 and 0.25 from SMAPVEX08 and the measurement points with VSM more than 0.25 from CLASIC. Additionally, the measurements over all fields with VWC less than 0.5 kg/m^2 have been plotted with red dots.

The results show that the measurements, both brightness temperature and normalized radar cross-section, from all campaigns form a consistent set of values responding to the in situ soil moisture. However, it is important to point out that the algorithms that actually retrieve the soil moisture from remotely sensed data account for surface temperature, surface roughness and vegetation. These plots are intended to only show the consistent trend of the airborne radar and radiometer measurements over all campaigns. Also, as expected, the soil moisture is more dominant in brightness temperature than in radar measurement which can be observed in higher dispersion in σ^0 value against the volumetric soil moisture.

4.3. Active vs. passive

In order to probe the relationship between the radiometer measured TB and radar measured σ^0 the same fields as above were used. Figure 9 shows TB values against σ^0 value over these fields (the black crosses). The red dots indicate the relationship over all fields with VWC less than 0.5 kg/m^2. As expected based on the previous results they correlate with each other. This relationship is essential for the combined active/passive soil moisture algorithms.

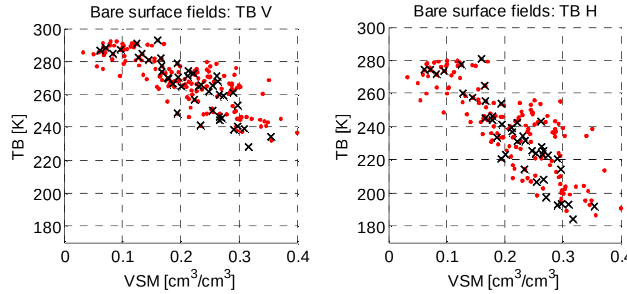

Figure 7. Brightness temperature for vertical (left) and horizontal (right) polarization as a function of in situ volumetric soil moisture over fields with nearly bare surfaces (crosses). Re dots show values for all fields with VWC < 0.5 kg/m^2.

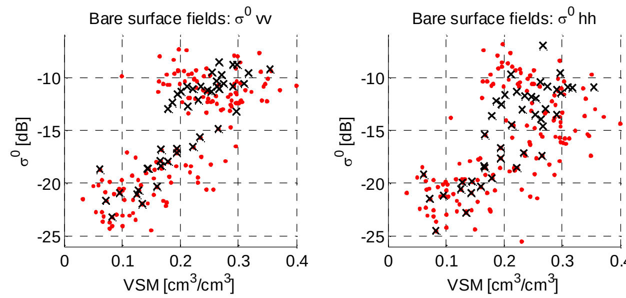

Figure 8. Vertically (left) and horizontally (right) co-polarized normalized radar cross-section as a function of in situ volumetric soil moisture over fields with nearly bare surfaces (crosses). Red dots show values for all fields with VWC < 0.5 kg/m^2.

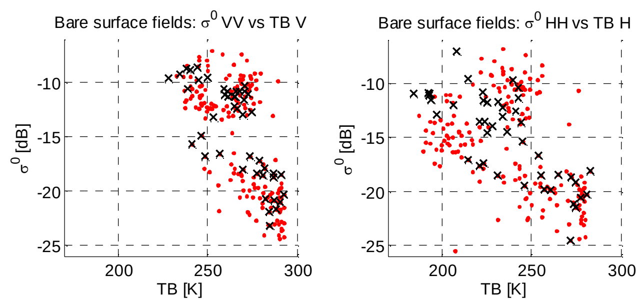

Figure 9. Vertically polarized NRCS against vertically polarized TB (left) and horizontally polarized NRCS against horizontally polarized TB over the low vegetation fields (crosses). Red dots show values for all fields with VWC < 0.5 kg/m^2.

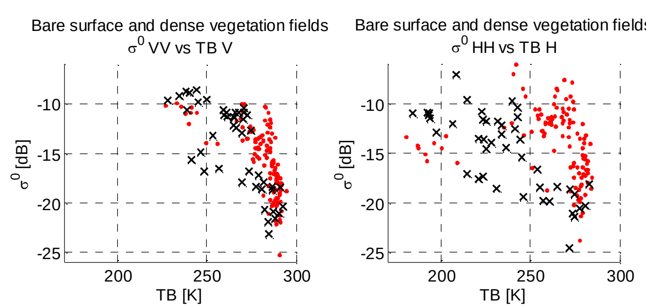

Figure 10. Vertically polarized NRCS against vertically polarized TB (left) and horizontally polarized NRCS against horizontally polarized TB over the low vegetation fields (crosses). Red dots show values for all fields with VWC in the range of 3 - 5 kg/m^2.

In the scatter plot the values from all low vegetation fields correspond well to the selected set of almost bare surface fields. Figure 10 shows the same selection of almost bare surface fields with the values for all fields with VWC between 3 kg/m^2 and 5 kg/m^2. As expected, the dynamic range of TB lowers with increasing VWC but the σ^0 experiences still high dynamic range due to the varying scattering processes associated with the structure of dense vegetation. In other words, the VWC parameter alone, which mostly represents the optical depth of the vegetation without addressing the structure, is not the only important parameter when relating σ^0 to TB.

5. DISCUSSION

The analyzed data feature wide range of soil moisture values with varying surface conditions. In the development of the SMAP retrieval algorithms the data from these experiments have already been utilized extensively to in part build the foundation for the science behind the mission. The data can be used to tune the parameterization and validate many basic aspects of the final retrieval algorithms before the launch of the mission.

In terms of the SMAP mission type measurement concept the data answers most needs of the radiometer soil moisture algorithm. However, wider range of vegetation types and density would be needed for fine tuning of the algorithm vegetation parameters for the diversity corresponding to global land cover.

The radar soil moisture algorithm is in general also fairly well served by the data set, although under denser vegetation conditions the radar algorithm modeling would require more detailed vegetation sampling to account for e.g. the vegetation structure.

The specialty of the SMAP, the combined radar/radiometer soil moisture retrieval, inherently benefits from the coincidental σ^0 and TB record. This record will be critical for the algorithm development and supplementing it with more data would be advantageous. The basic approach for utilizing the radar measurement for the combined algorithm is to disaggregate the coarser resolution radiometer measurement. Therefore, the spatially mapped data domains are crucial in exercising the disaggregation aspect of the algorithm. However, resolution scales more representative to SMAP measurement geometry will be important as the algorithm development moves forward. In order to also test time series schemes for the algorithm development it would be beneficial to have data sets spanning longer time periods such as in the case of CLASIC, for example.

Overall, all algorithms would benefit from additional vegetation and land cover type diversity. Especially, the data set could use replenishment of records with dense vegetation layer and land cover types other than agricultural.

6. CONCLUSIONS

The analyses presented in this paper show that the combined field campaign data set of SGP99, SMEX02, CLASIC and SMAPVEX08 campaigns utilizing the airborne PALS instrument provides a robust basis for soil moisture algorithm development for L-band radar and radiometer. The study suggests that there are also areas where the data set needs to be complemented to address the global diversity of land cover conditions. By investigating the historical data record the new data acquisitions can be designed to optimally supplement the available data set for the SMAP active and passive soil moisture algorithm development.

ACKNOWLEDGMENT

The research described in this publication was carried out at the Jet Propulsion Laboratory, California Institute of Technology, under a contract with the National Aeronautics and Space Administration.

REFERENCES

[1] Soil Moisture Active and Passive Mission, http://smap.jpl.nasa.gov, Jet Propulsion Laboratory, California Institute of Technology.

[2] W. Wilson, S. Yueh, S. Dinardo, S. Chazanoff, A. Kitiyakara, F. Li, Y. Rahmat-Samii, "Passive Active L- and S-Band (PALS) Microwave Sensor for Ocean Salinity and Soil Moisture Measurements", IEEE Trans. Geosci. Remote Sens., Vol. 39, No. 5, May 2001.

[3] http://disc.gsfc.nasa.gov/fieldexp/SGP99/

[4] http://nsidc.org/data/amsr_validation/soil_moisture/smex02/

[5] E. Njoku et al., "Observations of Soil Moisture Using a Passive and Active Low Frequency Microwave Airborne Sensor During SGP99", IEEE Trans. Geosci. Remote Sens., Vol. 40, No. 12, pp. 2659-2673, December 2002.

[6] J. Bolten, V. Lakshmi, E. Njoku, "Soil Moisture Retrieval Using the Passive/Active L- and S-band Radar/Radiometer", IEEE Trans. Geosci. Remote Sens., Vol. 41, No. 12, December 2003.

[7] U. Narayan, V. Lakshmi, E. Njoku, "Retrieval of Soil Moisture from Passive and Active L/S Band Sensor (PALS) Observations During the Soil Moisture Experiment in 2002 (SMEX02)", Remote Sens. Env., Vol. 92, pp. 483-496, 2004.

[8] S. Yueh, S. Dinardo, S. Chan, E. Njoku, T. Jackson, R. Bindlish, "Passive and Active L-Band System and Observations during the 2007 CLASIC Campaign", Proc. IEEE IGARSS08, Vol. 2, pp. II-241 - II-244, 7-11 July 2008.

[9] R. Bindlish, T. Jackson, R. Sun, M. Cosh, S. Yueh, S. Dinardo, "Combined Passive and Active Microwave Observations of Soil Moisture During CLASIC", IEEE Geosci. Remote Sens. Letters, Vol. 6, No. 4, October 2009.

[10] S. Yueh, S. Dinardo, S. Chan, E. Njoku, T. Jackson, R. Bindlish, J. Johnson, J. Piepmeier, C. Ruf, "PALS-ADD and Airborne Campaigns to Support Soil Moisture and Sea Surface Salinity Missions", Proc. IEEE IGARSS09, 12-17 July 2009.